frontiers | Frontiers in Chemistry

TYPE Original Research
PUBLISHED 03 June 2024
DOI 10.3389/fchem.2024.1411801

OPEN ACCESS

EDITED BY
Xuetao Xu,
Wuyi University, China

REVIEWED BY
Guanghao Zhu,
Shanghai University of Traditional Chinese Medicine, China
Danying Huang,
Guangdong University of Petrochemical Technology, China
Haoxing Zhang,
Shenzhen University, China

*CORRESPONDENCE
Faliang Liang,
faliang2024@163.com

RECEIVED 03 April 2024
ACCEPTED 16 May 2024
PUBLISHED 03 June 2024

CITATION
Liang F (2024), Inhibition mechanism investigation of quercetagetin as a potential tyrosinase inhibitor.
Front. Chem. 12:1411801.
doi: 10.3389/fchem.2024.1411801

Inhibition mechanism investigation of quercetagetin as a potential tyrosinase inhibitor

Faliang Liang*

Pharmacy Department, Jiang Men Maternity and Child Healthcare Hospital, Jiangmen, China

Tyrosinase is one important rate limiting enzyme in melanin synthesis, directly affecting the melanin synthesis. Quercetagetin is one active ingredient from marigold. Thence, the inhibition effects of quercetagetin against tyrosinase were investigated. The results showed quercetagetin could inhibit tyrosinase activity with IC_{50} value of 0.19 ± 0.01 mM and the inhibition type was a reversible mixed-type. Results of fluorescence quenching showed quercetagetin could quench tyrosinase fluorescence in static process. CD and 3D fluorescence results showed the interaction of quercetagetin to tyrosinase could change tyrosinase conformation to inhibit activity. Moreover, docking revealed details of quercetagetin's interactions with tyrosinase.

KEYWORDS

nature product, quercetagetin, tyrosinase, inhibition effects, inhibitor

1 Introduction

As we all know, various diseases affect people's health (Zhang et al., 2020; Zhang X. et al., 2021; Shi et al., 2023; Zhou S. et al., 2022). As a therapeutic target, tyrosinase is one important metal enzyme containing two copper, which widely presents in the organism (Min et al., 2023; Fan et al., 2017). Tyrosinase has been confirmed to be involved in the synthesis of melanin (Li et al., 2023; Hassan et al., 2023; Li J. et al., 2021). The first reaction process is monophenolase activity, in which L-tyrosine is hydroxylated into L-dopa and the second reaction process is diphenolase activity, in which L-dopa is subsequently oxidized into dopaquinone (Djafarou et al., 2023; Lee et al., 2023; Zargaham et al., 2023). In the organism, melanin acts crucial roles to protect the skin from UV radiation (Lu et al., 2023a; Znajafi et al., 2023). But, excessive elevated melanin content leads to lots of pigmentation disorders, including age spots and melanoma (Broulier et al., 2023; De Barros et al., 2023; Xue et al., 2023). Inhibition of tyrosinase activity would reduce melanin generation, thence, the finding on novel tyrosinase inhibitors is attracting more attention due to their potential application in medicine and cosmetics fields (Wang and Mu, 2021). Although kojic acid and arbutin (Figure 1) are applied as tyrosinase inhibitors in the medical and industrial fields, they still have been found to lots of adverse side effects (Wang et al., 2021; Esma et al., 2023). Now, to find novel tyrosinase inhibitors is essential for treatment of melanin synthesis (Romagnoli et al., 2022; Nasab et al., 2023).

Natural products have been the vital sources for clinical drugs (Li Y. et al., 2021; Wu et al., 2021; Chen et al., 2022; Zang et al., 2022). Many natural products display widely biological activities, such as antioxidant (Zhang Y. et al., 2021; Tao et al., 2022; Tang et al., 2023), anti-tumor (Liu et al., 2022; Chen et al., 2023; Song et al., 2023), anti-inflammatory (Wang et al., 2020; Wang X. et al., 2022; Zhou Y. et al., 2022), and so on (Wang Y. et al., 2022; Qi et al., 2022; Ma et al., 2023). In particular, natural products show low toxicity (Shao et al., 2020; Jiang et al., 2021;

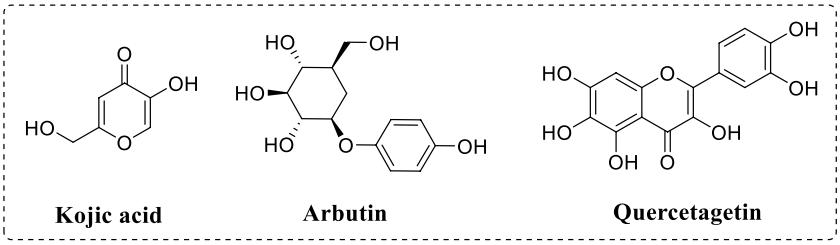

FIGURE 1
Chemical structure of kojic acid, arbutin and quercetagetin.

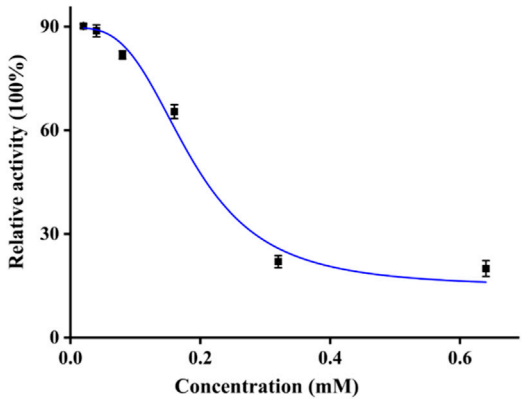

FIGURE 2
Tyrosinase inhibitory activity of quercetagetin.

Pei et al., 2021). Thence the development of natural products as tyrosinase inhibitors attracts much attention.

Quercetagetin (Figure 1) is one active ingredient from marigold and has a chemical structure of 3,3′,4′,5,6,7-hexahydroxyflavone (Bulut and Yilmaz, 2021; Wang X. et al., 2022). As one polyhydroxyphenol molecule with multiple hydrogen donor substituents, quercetagetin represents rich biological activities (Wu F. et al., 2023). For example, quercetagetin shows strong antioxidant activity and can effectively scavenge DPPH and ABTS (Fuentes et al., 2021). Quercetagetin also enhances the antioxidant enzymatic activities in broilers tissue by Nrf2/ARE signal pathway (Wu et al., 2022). In addition, quercetagetin displays immunomodulatory and anti-inflammatory to inhibit the release of macrophage-derived chemokine (Rufino et al., 2021). Besides, quercetagetin display other beneficial functions, including anti-virus and anti-diabetes (Seyedi et al., 2016). However, to our knowledge, the inhibition effects of quercetagetin against tyrosinase have not been reported yet.

Hence, in this study, we investigated the inhibition effects of quercetagetin against tyrosinase by the multispectral method, followed by the molecular docking.

2 Results and discussion

2.1 Inhibitory activity

The tyrosinase inhibitory activity of quercetagetin was examined on mushroom tyrosinase. The tyrosinase activity was measured under different concentrations of quercetagetin (Figure 2). It could be observed that tyrosinase relative activity gradually reduced with quercetagetin concentration (0–0.64 mM), meaning that quercetagetin could inhibit the tyrosinase activity with quercetagetin concentration. Its IC_{50} value was calculated to be 0.19 ± 0.01 mM, which was lower than that of kojic acid. This result showed that quercetagetin could be used as a natural tyrosinase inhibitor.

2.2 Kinetic study

There are two kinds of inhibitors, reversible and non-reversible inhibitors. For a reversible inhibitor, it can reduce the enzyme activity by the binding to enzyme, which can restore the enzyme activity through the remove of inhibitor. There are three reversible inhibitors, including competitive, non-competitive and mixed-type inhibitors. The inhibition type of quercetagetin on tyrosinase was subsequently investigated. With different concentration of quercetagetin and tyrosinase, the absorbance changes were measured (Figure 3A) and found that the lines of quercetagetin with different concentration passed origin and slopes reduced with quercetagetin concentration. The results suggested quercetagetin as a reversible inhibitor. With different concentration of quercetagetin and substrate, the absorbance changes were analyzed using Lineweaver-Burk plots (Figure 3B). The lines of quercetagetin intersected in the third quadrant and their slops increased with quercetagetin concentrations. The results indicated that quercetagetin inhibited tyrosinase in a mixed-type, meaning that quercetagetin bound to tyrosinase and tyrosinase-substrate complex to inhibit its activity. Similar phenomena were obtained in inhibition type of indole-carbohydrazides (Iraji et al., 2022).

Moreover, as shown in Figures 4A, B, the inhibition constants K_i and K_{is} were obtained from the secondary curves of inhibitory kinetics to be 0.24 and 0.12 mM. Smaller K_{is} value than K_i meant that binding force of quercetagetin with tyrosinase-substrate complex was stronger than with tyrosinase. That was to say that quercetagetin preferred to bind with tyrosinase-substrate complex.

2.3 Fluorescence quenching

The fluorescence quenching process of tyrosinase by quercetagetin was investigated. For fluorescence spectra of tyrosinase, they all showed characteristic peaks at 344 nm at 295,

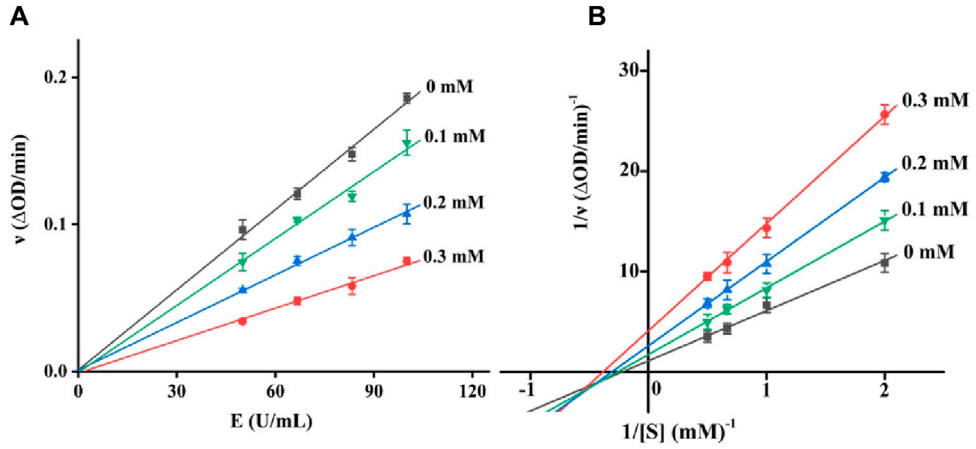

FIGURE 3
(A) Reversible assay of quercetagetin; **(B)** Lineweaver-Burk plots of quercetagetin.

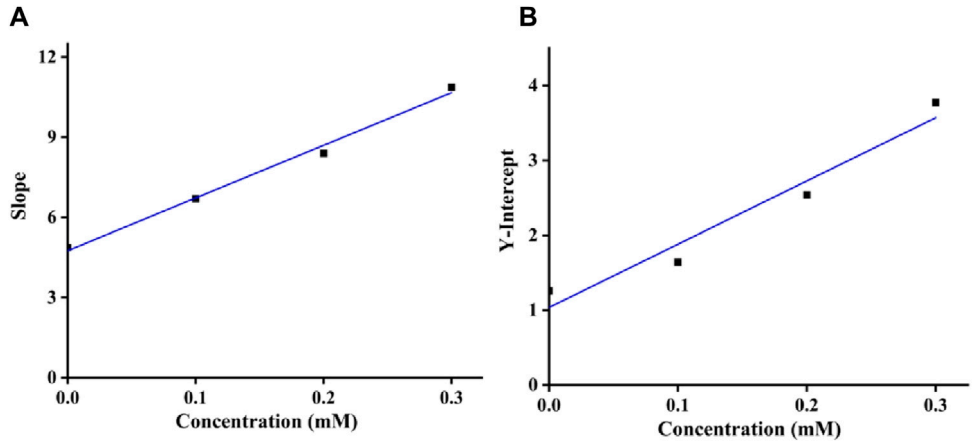

FIGURE 4
(A) K_i assay of quercetagetin; **(B)** K_{is} assay of quercetagetin.

298, and 305 K, respectively (Figures 5A–C). But, quercetagetin did not show effective fluorescence spectra. Moreover, when treated by quercetagetin, tyrosinase presented the gradually decreasing peak intensity (Figures 5A–C), which indicated that quercetagetin bound to tyrosinase.

The fluorescence quenching data at 295, 298, and 305 K were future analyzed by Stern-Volmer plots. As is shown in Figure 5D the Stern-Volmer plots of quercetagetin, lines with different temperature presented good linearity, meaning that there was only one quenching type of static or dynamic in quenching process. Then the quenching constant (K_{sv}) the bimolecular quench rate constant (K_q) were obtained (Table 1). The K_{sv} results found that K_{sv} values decreased with the temperature. And K_q values at 295, 298, and 305 K were higher than 2×10^{10} L mol^{-1} S^{-1}. Above results suggested the quenching process of quercetagetin against tyrosinase was a static process. This quenching type presented in the quenching of indole derivatives on α-glucosidase (Hu et al., 2024). The quenching process also was the process of thermodynamic changes. Thence, the thermodynamic parameters were calculated (Table 1). The negative ΔG value unlocked one spontaneous process of quercetagetin binding to tyrosinase. The positive ΔH and ΔS values suggested hydrophobic interactions as the important forces between quercetagetin and tyrosinase.

2.4 CD spectra

The effect of quercetagetin on conformation change of tyrosinase was investigated using CD spectra. Figure 6 showed CD spectra of tyrosinase, the characteristic peaks around 210–220 nm stood for the peptide chains of tyrosinase. When treated with quercetagetin, the CD spectra of tyrosinase appeared some changes, meaning its conformation change. Then its secondary structure contents were calculated (Table 2) and found that quercetagetin treatment (molar ratio: 2:1) caused reduction of

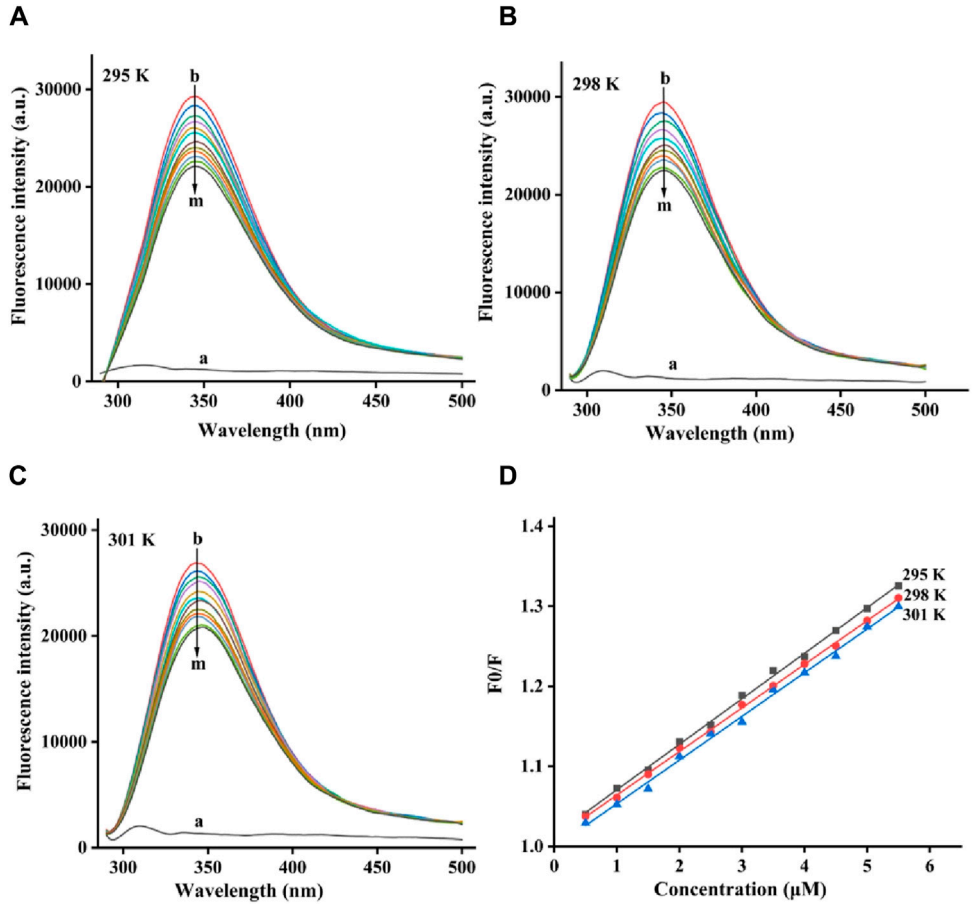

FIGURE 5
(A–C) Fluorescence quenching spectra of quercetagetin on tyrosinase at 295, 298, and 305 K, respectively; **(D)** Stern-Volmer plots of quercetagetin.

TABLE 1 Parameters of quercetagetin with tyrosinase.

T (K)	K_q (x10^{12} $Lmol^{-1}S^{-1}$)	K_{sv} (x$10^4 Lmol^{-1}$)	△H (KJ/moL)	△G (KJ/moL)	△S (J/(mol·K)
295	5.69	5.69	25.34	−23.27	164.78
298	5.45	5.45		−23.76	
301	5.40	5.40		−24.26	

α-helix and random coils and increase of β-sheet and β-turn. These results indicated that quercetagetin treatment could lead to conformation changes of tyrosinase.

2.5 3D fluorescence spectra

3D fluorescence spectra were monitored to further investigate the effect on conformation of tyrosinase by quercetagetin. As shown in Figure 7A the 3D fluorescence spectra tyrosinase, two characteristic peaks appeared, including Peak A for Tyr and Trp residues and Peak B for peptide backbone. When treated with quercetagetin, Peak A and Peak B were reduced the intensity by 35.4% and 13.3%, respectively (Figure 7B), which suggested that quercetagetin treatment would cause the changes of Tyr and Trp residues, and peptide backbone. That was to say that quercetagetin treatment would cause the conformation change of tyrosinase.

2.6 Molecular docking

The interaction of quercetagetin to tyrosinase was simulated by molecular docking method. As shown in Figure 8A the docking results, quercetagetin bound to the active pocket of tyrosinase with trihydroxychromone section in the active catalytic zone of active pocket. From Figure 8B the docking results in detail, it could be observed that quercetagetin made one hydrogen bond with His259 and hydrophobic interaction with Val248, His263, Val283, and Ala286. The results indicated that the interactions

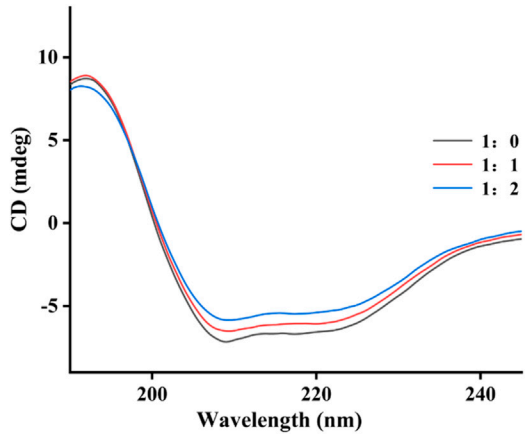

FIGURE 6
CD spectra of tyrosinase with quercetagetin.

between quercetagetin and tyrosinase resulted in the reduction of tyrosinase activity.

2.7 Copper-chelating activity

The copper-chelating activity of quercetagetin was finally assayed using copper sulfate. Figure 9A showed the quercetagetin-copper sulfate mixture. Quercetagetin showed its UV spectra with characteristic peak at 370 nm. While, after added copper sulfate, the UV characteristic peak of quercetagetin was gradually decreased. These results indicated that copper might complex with quercetagetin to change its UV characteristic peak. The peak intensity at different molar ratios of quercetagetin to copper sulfate was analyzed (Figure 9B) and found that the decreasing trend of quercetagetin peak intensity become equilibrium, meaning that the binding molar ratio of quercetagetin with copper sulfate was 1. The copper-chelating activity of quercetagetin also might be one reason of the reduction of tyrosinase activity.

3 Conclusion

Tyrosinase is one important rate limiting enzyme in melanin synthesis, directly affecting the melanin synthesis. Quercetagetin is one active ingredient from marigold. In this study, the inhibition effects of quercetagetin against tyrosinase were investigated. The results showed that quercetagetin could inhibit the tyrosinase activity with IC_{50} value of 0.19 ± 0.01 mM and the inhibition type was a reversible mixed-type. Results of fluorescence quenching showed that quercetagetin could quench tyrosinase fluorescence in static process. CD and 3D fluorescence results showed interaction of quercetagetin to tyrosinase could change tyrosinase conformation to inhibit activity. Moreover, docking revealed details of quercetagetin's interactions with tyrosinase.

4 Materials and methods

4.1 Tyrosinase activity assay

Tyrosinase inhibitory activity of quercetagetin was measured (Lu et al., 2023b). 10 μL of quercetagetin in DMSO solutions was added into 140 μL of tyrosinase in PBS solution and incubated for

TABLE 2 The secondary structure contents of tyrosinase with quercetagetin.

Molar ratio	α-Helix (%)	β-Sheet (%)	β-Turn (%)	Random coils (%)
1:0	27.0	23.1	15.6	44.7
1:1	22.2	27.6	16.9	41.1
1:2	19.2	31.4	17.9	38.8

Note: Molar ratio means [tyrosinase]: [quercetagetin].

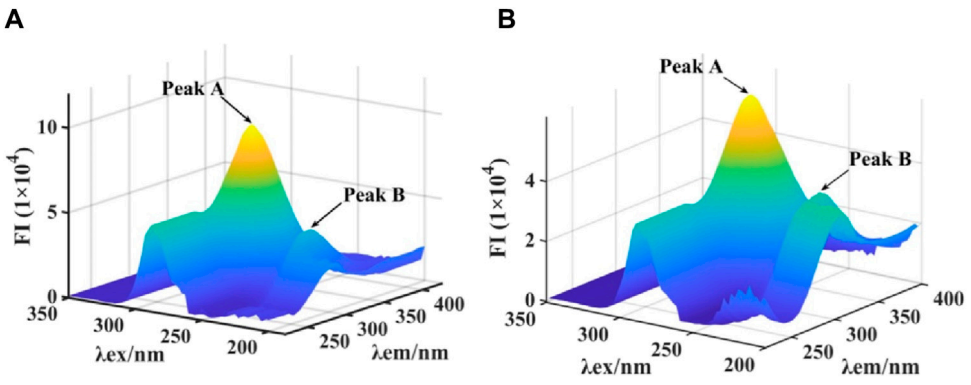

FIGURE 7
(A,B) 3D fluorescence of tyrosinase and quercetagetin-tyrosinase, respectively.

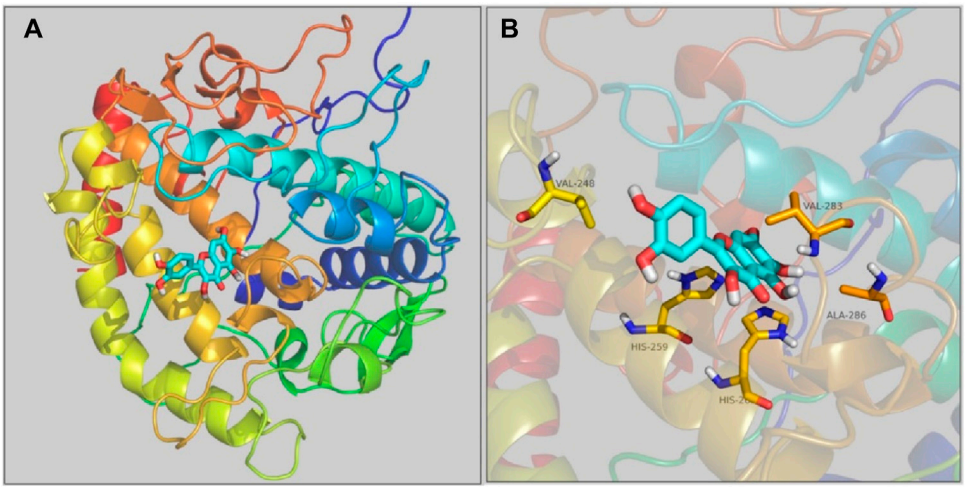

FIGURE 8
(A,B) The molecular docking of quercetagetin to tyrosinase.

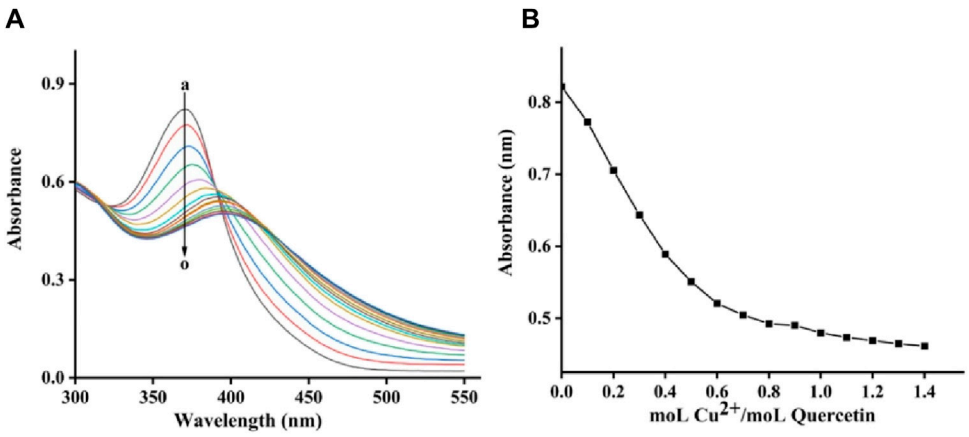

FIGURE 9
(A) UV spectra of quercetagetin-copper sulfate mixture; **(B)** UV peak of quercetagetin versus molar ratios of quercetagetin to copper sulfate.

10 min. 50 μL of L-dopa (in PBS) was added as the substrates. Then, the absorbance was measured at 475 nm on a microplate reader. Kojic acid was selected as the positive control. All experiments were tested in triplicate. Inhibition rate (%) = $[(OD_1\text{-}OD_0)/OD_0]\times100\%$. OD_0 and OD_1 were the absorbance of tyrosinase and tyrosinase-quercetagetin mixture.

4.2 Inhibitory kinetics

The reversibility of quercetagetin against tyrosinase was analyzed at different concentration of quercetagetin with tyrosinase or L-dopa. And the inhibitory kinetics of quercetagetin against tyrosinase was analyzed at different concentration of quercetagetin with tyrosinase or L-dopa. The inhibition constants K_i and K_{is} were obtained from the secondary curves of inhibitory kinetics (Xu et al., 2020; Deng et al., 2022; Lin et al., 2023).

4.3 Fluorescence quenching

To the 3.0 mL of tyrosinase solution, 1 μL of quercetagetin was added by titration method (Li et al., 2024a; Min et al., 2024). The mixture was measured fluorescence spectra at excitation of 280 nm. The experiments were conducted at temperatures of 295, 298, and 305 K, respectively. The Stern-Volmer equation and the van't Hoff equation were employed to obtained parameters.

4.4 CD spectra

To the 100 μL of tyrosinase solution, 1 μL of quercetagetin was added. CD spectra were measured at room temperature (Xiao et al., 2023; Li et al., 2024b). Tyrosinase solution without quercetagetin was also measured its CD spectra.

4.5 3D fluorescence spectra

To the 3.0 mL of tyrosinase solution, 1 μL of quercetagetin was added. 3D fluorescence spectra were measured (Wu X. et al., 2023).

4.6 Copper-chelating activity

To the 2 mL of quercetagetin solution, 5 μL of copper sulfate solution was gradually added. UV absorption spectra were detected. The molar ratios of quercetagetin to copper sulfate ranged from 10: 0 to 10: 14.

4.7 Molecular docking

Docking of quercetagetin with tyrosinase was simulated using the SYBYL software (Zhang et al., 2022; Feng et al., 2024). The tyrosinase crystal structure (PDB: 2Y9X) was optimized by removing water, adding hydrogen, and generation of active pocket. Quercetagetin structure was performed energy minimization. Thence, docking procedure was run in the default format.

Data availability statement

The raw data supporting the conclusion of this article will be made available by the authors, without undue reservation.

Author contributions

FL: Conceptualization, Investigation, Methodology, Project administration, Writing–original draft, Writing–review and editing.

Funding

The author(s) declare that no financial support was received for the research, authorship, and/or publication of this article.

Conflict of interest

The author declares that the research was conducted in the absence of any commercial or financial relationships that could be construed as a potential conflict of interest.

Publisher's note

All claims expressed in this article are solely those of the authors and do not necessarily represent those of their affiliated organizations, or those of the publisher, the editors and the reviewers. Any product that may be evaluated in this article, or claim that may be made by its manufacturer, is not guaranteed or endorsed by the publisher.

References

Broulier, R. I., Lazinski, L. M., Pérès, B., Olleik, H., Royal, G., Fishman, A., et al. (2023). Resorcinol-based hemiindigoid derivatives as human tyrosinase inhibitors and melanogenesis suppressors in human melanoma cells. *Eur. J. Med. Chem.* 246, 114972. doi:10.1016/j.ejmech.2022.114972

Bulut, O., and Yilmaz, M. D. (2021). Concise synthesis of quercetagetin (3,3',4',5,6,7-hexahydroxyflavone) with antioxidant and antibacterial activities. *Results Chem.* 3, 100255. doi:10.1016/j.rechem.2021.100255

Chen, J., Cao, D., Jiang, S., Liu, X., Pan, W., Cui, H., et al. (2022). Triterpenoid saponins from Ilex pubescens promote blood circulation in blood stasis syndrome by regulating sphingolipid metabolism and the PI3K/AKT/eNOS signaling pathway. *Phytomedicine* 104, 154242. doi:10.1016/j.phymed.2022.154242

Chen, Y., Yin, S., Liu, R., Yang, Y., Wu, Q., Lin, W., et al. (2023). β-Sitosterol activates autophagy to inhibit the development of hepatocellular carcinoma by regulating the complement C5a receptor 1/alpha fetoprotein axis. *Eur. J. Pharmacol.* 957, 175983. doi:10.1016/j.ejphar.2023.175983

De Barros, M. R., Menezes, T. M., Garcia, Y. S., and Neves, J. L. (2023). Inhibitory effects of iron-based carbonaceous nanocomposites on mushroom tyrosinase activity: molecular aspects and mechanistic insights. *New J. Chem.* 47, 9134–9142. doi:10.1039/d3nj00882g

Deng, X., Ke, J., Zheng, Y., Li, D., Zhang, K., Zheng, X., et al. (2022). Synthesis and bioactivities evaluation of oleanolic acid oxime ester derivatives as α-glucosidase and a-amylase inhibitors. *J. Enzyme Inhib.* 37, 451–461. doi:10.1080/14756366.2021.2018682

Djafarou, S., Mermer, A., Barut, B., Yılmaz, G. T., Khodja, I. A., and Boulebd, H. (2023). Synthesis and evaluation of the antioxidant and anti-tyrosinase activities of thiazolyl hydrazone derivatives and their application in the anti-browning of fresh-cut potato. *Food Chem.* 414, 135745. doi:10.1016/j.foodchem.2023.135745

Esma, A. T. K., Abd, E. H. K., Rabah, A., Djamila, B., Mohamed, S. B., Chawki, B., et al. (2023). *In vitro* assessment of antioxidant, neuroprotective, anti-urease and anti-tyrosinase capacities of Tamarix africana leaves extracts. *J. Tradit. Chin. Med.* 43, 252–264. doi:10.19852/j.cnki.jtcm.20230105.003

Fan, M., Zhang, G. W., Pan, J., and Gong, D. (2017). An inhibition mechanism of dihydromyricetin on tyrosinase and the joint effects of vitamins B6, D3 or E. *Food Funct.* 8, 2601–2610. doi:10.1039/c7fo00236j

Feng, M., Liang, B., Sun, J., Min, X., Wang, S., Lu, Y., et al. (2024). Synthesis, anti-α-glucosidase activity, inhibition interaction, and anti-diabetic activity of novel cryptolepine derivatives. *J. Mol. Struct.* 1310, 138311. doi:10.1016/j.molstruc.2024.138311

Fuentes, J., de Camargo, A. C., Atala, E., Gotteland, M., Olea-Azar, C., and Speisky, H. (2021). Quercetin oxidation metabolite present in onion peel protects caco-2 cells against the oxidative stress, NF-kB activation, and loss of epithelial barrier function induced by NSAIDs. *J. Agric. Food Chem.* 69, 2157–2167. doi:10.1021/acs.jafc.0c07085

Hassan, M., Shahzadi, S., and Kloczkowski, A. (2023). Tyrosinase inhibitors naturally present in plants and synthetic modifications of these natural products as anti-melanogenic agents: a review. *Molecules* 28, 378. doi:10.3390/molecules28010378

Hu, C., Liang, B., Sun, J., Li, J., Xiong, Z., Wang, S., et al. (2024). Synthesis and biological evaluation of indole derivatives containing thiazolidine-2,4-dione as α-glucosidase inhibitors with antidiabetic activity. *Eur. J. Med. Chem.* 264, 115957. doi:10.1016/j.ejmech.2023.115957

Iraji, A., Sheikhi, N., Attarroshan, M., Ardani, G. R. S., Kabiri, M., Bafghi, A. N., et al. (2022). Design, synthesis, spectroscopic characterization, *in vitro* tyrosinase inhibition, antioxidant evaluation, *in silico* and kinetic studies of substituted indole-carbohydrazides. *Bioorg. Chem.* 129, 106140–140. doi:10.1016/j.bioorg.2022.106140

Jiang, T., Ji, C., Cheng, X., Gu, S., Wang, R., Li, Y., et al. (2021). α-Mangostin alleviated HIF-1α-mediated angiogenesis in rats with adjuvant-induced arthritis by suppressing aerobic glycolysis. *Front. Pharmacol.* 12, 785586. doi:10.3389/fphar.2021.785586

Lee, J., Park, Y. J., Jung, H. J., Ullah, S., Yoon, D., Jeong, Y., et al. (2023). Design and synthesis of (Z)-2-(benzylamino)-5-benzylidenethiazol-4(5H)-one derivatives as tyrosinase inhibitors and their anti-melanogenic and antioxidant effects. *Molecules* 28, 848. doi:10.3390/molecules28020848

Li, J., Feng, L., Liu, L., Wang, F., Ouyang, L., Zhang, L., et al. (2021a). Recent advances in the design and discovery of synthetic tyrosinase inhibitors. *Eur. J. Med. Chem.* 224, 113744. doi:10.1016/j.ejmech.2021.113744

Li, J., Min, X., Zheng, X., Wang, S., Xu, X., and Peng, J. (2023). Synthesis, anti-tyrosinase activity, and spectroscopic inhibition mechanism of cinnamic acid-eugenol esters. *Molecules* 28, 5969. doi:10.3390/molecules28165969

Li, M., Li, H., Min, X., Sun, J., Liang, B., Xu, L., et al. (2024a). Identification of 1,3,4-thiadiazolyl-containing thiazolidine-2,4-dione derivatives as novel PTP1B inhibitors with anti-diabetic activity. *J. Med. Chem.* doi:10.1021/acs.jmedchem.4c00676

Li, M., Sun, J., Liang, B., Min, X., Hu, J., Wu, R., et al. (2024b). Thiazolidine-2,4-dione derivatives as potential α-glucosidase inhibitors: synthesis, inhibitory activity, binding

interaction and hypoglycemic activity. *Bioorg. Chem.* 144, 107177. doi:10.1016/j.bioorg.2024.107177

Li, Y., Dai, M., Wang, L., and Wang, G. (2021b). Polysaccharides and glycosides from Aralia echinocaulis protect rats from arthritis by modulating the gut microbiota composition. *J. Ethnopharmacol.* 269, 113749. doi:10.1016/j.jep.2020.113749

Lin, J., Xiao, D., Lu, L., Liang, B., Xiong, Z., and Xu, X. (2023). New β-carboline derivatives as potential α-glucosidase inhibitor: synthesis and biological activity evaluation. *J. Mol. Struct.* 1283, 135279. doi:10.1016/j.molstruc.2023.135279

Liu, J., Zhao, X., Qin, F., Zhou, J., Ding, F., Zhou, G., et al. (2022). Isoliquiritigenin mitigates oxidative damage after subarachnoid hemorrhage *in vivo* and *in vitro* by regulating Nrf2-dependent Signaling Pathway via Targeting of SIRT1. *Phytomedicine* 105, 154262. doi:10.1016/j.phymed.2022.154262

Lu, L., Hu, C., Min, X., Liu, Z., Xu, X., and Gan, L. (2023a). *In vitro* and *in vivo* biological evaluation of indole-thiazolidine-2,4-dione derivatives as tyrosinase inhibitors. *Molecules* 28, 7470. doi:10.3390/molecules28227470

Lu, L., Zhang, X., Kang, Y., Xiong, Z., Zhang, K., Xu, X., et al. (2023b). Novel coumarin derivatives as potential tyrosinase inhibitors: synthesis, binding analysis and biological evaluation. *Arab. J. Chem.* 16, 104724. doi:10.1016/j.arabjc.2023.104724

Ma, M., Wei, N., Yang, J., Ding, T., Song, A., Chen, L., et al. (2023). Schisandrin B promotes senescence of activated hepatic stellate cell *via* NCOA4-mediated ferritinophagy. *Pharm. Biol.* 61, 621–629. doi:10.1080/13880209.2023.2189908

Min, X., Guo, S., Lu, Y., and Xu, X. (2024). Investigation on the inhibition mechanism and binding behavior of cryptolepine to α-glucosidase and its hypoglycemic activity by multi-spectroscopic method. *J. Lumin.* 269, 120437. doi:10.1016/j.jlumin.2024.120437

Min, X., Lu, L., Xu, X. T., Wen, Y., and Zheng, X. (2023). Investigation on the inhibition mechanism and binding behavior of paeonol to tyrosinase and its anti-browning property by multi-spectroscopic and molecular docking methods. *Int. J. Biol. Macromol.* 253, 126962. doi:10.1016/j.ijbiomac.2023.126962

Nasab, N., Raza, H., Eom, Y., Hassan, M., Kloczkowski, A., and Kim, S. (2023). Synthesis and discovery of potential tyrosinase inhibitor of new coumarin-based thiophenyl-pyrazolylthiazole nuclei: in-vitro evaluation, cytotoxicity, kinetic and computational studies. *Chem. Biol. Drug. Des.* 101, 13–88. doi:10.1111/cbdd.14209

Pei, Y. Q., Zheng, Y. Q., Ding, Y. D., Xu, Q. X., Cao, D., Wu, Y. N., et al. (2021). Triptolide attenuates vascular calcification by upregulating expression of miRNA-204. *Front. Pharmacol.* 11, 581230. doi:10.3389/fphar.2020.581230

Qi, X., Zheng, S., Ma, M., Lian, N., Wang, H., Chen, L., et al. (2022). Curcumol suppresses CCF-mediated hepatocyte senescence through blocking LC3B-Lamin B1 interaction in alcoholic fatty liver disease. *Front. Pharmacol.* 13, 912825. doi:10.3389/fphar.2022.912825

Romagnoli, R., Oliva, P., Prencipe, F., Manfredini, S., Germanò, M., De Luca, L., et al. (2022). Cinnamic acid derivatives linked to arylpiperazines as novel potent inhibitors of tyrosinase activity and melanin synthesis. *Eur. J. Med. Chem.* 231, 114147. doi:10.1016/j.ejmech.2022.114147

Rufino, A. T., Ramalho, A., Sousa, A., de Oliveira, J. M. P. F., Freitas, P., Gómez, M. A. G., et al. (2021). Protective role of flavonoids against intestinal pro-inflammatory effects of silver nanoparticles. *Molecules* 26, 6610. doi:10.3390/molecules26216610

Seyedi, S. S., Shukri, M., Hassandarvish, P., Oo, A., Shankar, E. M., Abubakar, S., et al. (2016). Computational approach towards exploring potential anti-chikungunya activity of selected flavonoids. *Sci. Rep.* 6, 24027. doi:10.1038/srep24027

Shao, X., Li, B., Shen, J., Wang, Q., Chen, S., Jiang, X., et al. (2020). Ghrelin alleviates traumatic brain injury-induced acute lung injury through pyroptosis/NF-κB pathway. *Int. Immunopharmacol.* 79, 106175. doi:10.1016/j.intimp.2019.106175

Shi, L., Jiang, C., Xu, H., Wu, J., Lu, J., He, Y., et al. (2023). Hyperoside ameliorates cerebral ischaemic–reperfusion injury by opening the TRPV4 channel *in vivo* through the IP 3-PKC signalling pathway. *Pharm. Biol.* 61, 1000–1012. doi:10.1080/13880209.2023.2228379

Song, A., Ding, T., Wei, N., Yang, J., Ma, M., Zheng, S., et al. (2023). Schisandrin B induces HepG2 cells pyroptosis by activating NK cells mediated anti-tumor immunity. *Toxicol. Appl. Pharmacol.* 472, 116574. doi:10.1016/j.taap.2023.116574

Tang, Z., Zhang, M., Gao, L., Bao, Y., Li, P., Wang, M., et al. (2023). Optimal extraction of polysaccharides from Stevia rebaudiana roots for protection against hydrogen peroxide-induced oxidative damage in RAW264.7 cells. *Nat. Prod. Res.* 2023, 2263905. doi:10.1080/14786419.2023.2263905

Tao, Z. S., Li, T. L., and Wei, S. (2022). Silymarin prevents iron overload induced bone loss by inhibiting oxidative stress in an ovariectomized animal model. *Chem. Biol. Interact.* 366, 110168. doi:10.1016/j.cbi.2022.110168

Wang, D., Li, Y., Wu, Y., Wu, Y., Han, J., Olatunji, O., et al. (2021). Xanthones from Securidaca inappendiculata antagonized the antirheumatic effects of methotrexate *in vivo* by promoting its secretion into urine. *Expert Opin. Drug Metab. toxico.* 17, 241–250. doi:10.1080/17425255.2021.1843634

Wang, L., Wang, P., Wang, D., Tao, M., Xu, W., and Olatunji, O. J. (2020). Anti-inflammatory activities of kukoamine A from the root bark of lycium chinense miller. *Nat. Prod. Commun.* 15, 1934578X2091208. doi:10.1177/1934578x20912088

Wang, R., and Mu, J. (2021). Arbutin attenuates ethanol-induced acute hepatic injury by the modulation of oxidative stress and Nrf-2/HO-1 signaling pathway. *J. Biochem. Mol. Toxicol.* 35, 22872. doi:10.1002/jbt.22872

Wang, X., Zhou, D., Zhou, W., Liu, J., Xue, Q., Huang, Y., et al. (2022a). Clematichinenoside AR inhibits the pathology of rheumatoid arthritis by blocking the circPTN/miR-145-5p/FZD4 signal axis. *Int. Immunopharm.* 113, 109376. doi:10.1016/j.intimp.2022.109376

Wang, Y., Wu, H., Han, Z., Sheng, H., Wu, Y., Wang, Y., et al. (2022b). Guhong injection promotes post-stroke functional recovery via attenuating cortical inflammation and apoptosis in subacute stage of ischemic stroke. *Phytomedicine* 99, 154034. doi:10.1016/j.phymed.2022.154034

Wu, F., Wang, F., Tang, Z., Yang, X., Liu, Y., Zhao, M., et al. (2023a). Quercetagetin alleviates zearalenone-induced liver injury in rabbits through Keap1/Nrf2/ARE signaling pathway. *Front. Pharmacol.* 14, 1271384. doi:10.3389/fphar.2023.1271384

Wu, F., Wang, H., Li, S., Wei, Z., Han, S., and Chen, B. (2022). Effects of dietary supplementation with quercetagetin on nutrient digestibility, intestinal morphology, immunity, and antioxidant capacity of broilers. *Front. Vet. Sci.* 9, 1060140. doi:10.3389/fvets.2022.1060140

Wu, X., Zhu, W., Lu, L., Hu, C., Zheng, Y., Zhang, X., et al. (2023b). Synthesis and anti-α-glucosidase activity evaluation of betulinic acid derivatives. *Arab. J. Chem.* 16, 104659. doi:10.1016/j.arabjc.2023.104659

Wu, Z., Liang, D., Xu, M., Liu, Y., and Xie, H. (2021). A comparative pharmacokinetic study of schisandrol B after oral administration of schisandrol b monomer and schisandra chinensis extract. *Curr. Pharm. Anal.* 17, 273–284. doi:10.2174/1573412916666191114122101

Xiao, D., Lu, L., Liang, B., Xiong, Z., Xu, X., and Chen, W. (2023). Identification of 1,3,4-oxadiazolyl-containing β-carboline derivatives as novel α-glucosidase inhibitors with antidiabetic activity. *Eur. J. Med. Chem.* 261, 115795. doi:10.1016/j.ejmech.2023.115795

Xu, X., Deng, X., Chen, J., Liang, Q., Zhang, K., Li, D., et al. (2020). Synthesis and biological evaluation of coumarin derivatives as aglucosidase Inhibitors. *Eur. J. Med. Chem.* 112, 112013. doi:10.1016/j.ejmech.2019.112013

Xue, S., Li, Z., Ze, X., Wu, X., He, C., Shuai, W., et al. (2023). Design, synthesis, and biological evaluation of novel hybrids containing dihydrochalcone as tyrosinase inhibitors to treat skin hyperpigmentation. *J. Med. Chem.* 66, 5099–5117. doi:10.1021/acs.jmedchem.3c00012

Zang, L., Xu, H., Huanh, C., Wang, C., Wang, R., Chen, R., et al. (2022). A link between chemical structure and biological activity in triterpenoids. *Recent Pat. Anti-Canc* 17, 145–161. doi:10.2174/1574892816666210512031635

Zargaham, M. K., Ahmed, M., Akhtar, N., Ashraf, Z., Abdel-Maksoud, M. A., Aufy, M., et al. (2023). Synthesis, *in silico* studies, and antioxidant and tyrosinase inhibitory potential of 2-(substituted phenyl) thiazolidine-4-carboxamide derivatives. *Pharmaceuticals* 16, 835. doi:10.3390/ph16060835

Zhang, X., Lu, Y., Li, W., Tao, T., Peng, L., Wang, W., et al. (2021a). Astaxanthin ameliorates oxidative stress and neuronal apoptosis via SIRT1/NRF2/Prx2/ASK1/p38 after traumatic brain injury in mice. *Brit. J. Pharmacol.* 178, 1114–1132. doi:10.1111/bph.15346

Zhang, X., Peng, L., Zhang, J., Dong, Y. P., Wang, C. J., Liu, C., et al. (2020). Berberine ameliorates subarachnoid hemorrhage injury via induction of sirtuin 1 and inhibiting HMGB1/Nf-κB pathway. *Front. Pharmacol.* 11, 1073. doi:10.3389/fphar.2020.01073

Zhang, X., Zheng, Y., Hu, C., Wu, X., Lin, J., Xiong, Z., et al. (2022). Synthesis and biological evaluation of coumarin derivatives containing oxime ester as α-glucosidase inhibitors. *Arab. J. Chem.* 15, 104072. doi:10.1016/j.arabjc.2022.104072

Zhang, Y., Zhang, X., Li, H. J., Zhou, T. F., Zhou, A. C., Zhong, Z. L., et al. (2021b). Antidepressant-like effects of helicid on a chronic unpredictable mild stress-induced depression rat model: inhibiting the IKK/IκBα/NF-κB pathway through NCALD to reduce inflammation. *Int. Immunopharm.* 93, 107165. doi:10.1016/j.intimp.2020.107165

Zhou, S., Sun, Y., Xing, Y., Wang, Z., Wan, S., Yao, X., et al. (2022a). Exenatide ameliorates hydrogen peroxide-induced pancreatic β-cell apoptosis through regulation of METTL3-mediated m6A methylation. *Eur. J. Pharmacol.* 924, 174960. doi:10.1016/j.ejphar.2022.174960

Zhou, Y., Xiang, R., Qin, G., Ji, B., Yang, S., Wang, G., et al. (2022b). Xanthones from *Securidaca inappendiculata Hassk.* attenuate collagen-induced arthritis in rats by inhibiting the nicotinamide phosphoribosyltransferase/glycolysis pathway and macrophage polarization. *Int. Immunopharm.* 111, 109137. doi:10.1016/j.intimp.2022.109137

Znajafi, E. A., Chehardoli, G., Ziaei, M., Akbarzadeh, T., Saeedi, M., Gholamhoseini, P., et al. (2023). Design, synthesis, *in vitro*, and *in silico* studies of novel benzylidene 6-methoxy-1-tetralone linked to benzyloxy and benzyl-1, 2, 3-triazole rings as potential tyrosinase inhibitors. *J. Mol. Struct.* 1271, 134018. doi:10.1016/j.molstruc.2022.134018